Spectroscopic and Theoretical Determination of the Electronic Structure of Anisole, Thioanisole, and Methoxy- and Methylthiobenzonitriles: A Contribution to the Study of Organic Conducting Polymers

Maurizio Dal Colle and Giuseppe Distefano*

Dipartimento di Chimica, Università di Ferrara, via Borsari 46, 44100 Ferrara, Italy

Derek Jones

ICoCEA, Consiglio Nazionale delle Ricerche, via Gobetti 101, 40129 Bologna, Italy

Alberto Modelli

Dipartimento di Chimica "G. Ciamician", Università di Bologna, via Selmi 2, 40126 Bologna, Italy

Received: February 1, 2000; In Final Form: May 25, 2000

Gas-phase ionization and attachment energy (IE and AE) values of some *p*- and *o*-cyano derivatives of anisole and thioanisole (*p*-NCPhXCH$_3$, X = O, S; and *o*-NCPhXR, X = O, R = CH$_3$; X = S, R = H, CH$_3$, and C(CH$_3$)$_3$) have been determined experimentally. The assignments of the spectra, based on those of the parent compounds PhXMe, NCPh, and XMe$_2$ (Me = CH$_3$), agree with the results of theoretical HF/6-31G** calculations. The calculations correctly reproduce the prevalence of the planar rotamer of the oxy derivatives with respect to the gauche one, while overestimating the relative stability of the gauche conformer of the thio derivatives. The two rotamers of the thio derivatives have similar energy and their valence energy levels do not sizably differ. In addition, PhSMe and *p*-NCPhSMe have HOMO−LUMO energy gaps (<9.0 eV) smaller than the corresponding value (>9.5 eV) in the oxy derivatives and there are indications that the methylthio group has larger polarizability than the methoxy group. These data suggest that poly(*p*-phenylene sulfide) is more suitable than poly(*p*-phenylene oxide) to carry electricity under mild doping.

Introduction

Over the past few years the geometric and electronic structures of heteroaromatic monomer and oligomer precursors of polymers whose electrical conductivity increases when properly ionized (p- or n-doped)[1−9] have been widely studied to elucidate structure−property relationships. In particular, we have studied oligothiophenes,[10] oligofurans,[11] and methyl-,[12] methylchalcogeno-,[13] and carbonyl-substituted[14,15] thiophenes using a multidisciplinary approach based on ultraviolet photoelectron (UP) and electron transmission (ET) spectroscopies and theoretical calculations.

Poly(*p*-arylene chalcogenide)s constitute another interesting class of conducting polymers. Poly(*p*-phenylene sulfide), PPS, is a processable and commercially available polymer which has a variety of uses as a thermoplastic. Consecutive phenyl rings of PPS are inclined alternately by +45° and −45° with respect to the planar zigzag chain of the sulfur atoms.[16−18] It has been alternatively proposed that two consecutive phenyl rings are nearly coplanar with the C−S−C plane with neighboring rings inclined at about 60°.[19] In both cases, π-conjugation along the polymer chain should not be very large. Nevertheless, optical dichroism measurements indicate[20] that the lowest lying optical transition of PPS is parallel to the polymer backbone. This requires[21] interaction of phenyl π-orbitals with sulfur p-orbitals as indicated by oligomer[22] and polymer calculations.[23]

PPS can be p-doped with AsF_5 under mild conditions giving rise, presumably, to a conductive charge-transfer complex with AsF_6^- as the anion (electrical conductivity, σ, 10^{-2}−1 S/cm[24,25]). Films of AsF_5-doped PPS cast from AsF_3 solution exhibit higher conductivities (25−200 S/cm), ascribed to irreversibly modified polymers.[21,26]

Poly(*p*-phenylene oxide), PPO, experiences a similar dramatic increase in electrical properties as a result of solution processing, namely from $<10^{-3}$ S/cm with solid state doping to 10^2 S/cm with solution casting.[21,26] PPO and its precursors, however, have been much less investigated.[27] The doping process under mild conditions has been reported to give rise to polymers with much smaller σ values than PPS doped under the same conditions,[26,27] that is, where irreversible chemical reactions (involving C−C bond formation) do not occur. The different behavior of oxygen-containing polymers with respect to the corresponding sulfur derivatives is not yet well understood.[4,11]

In this paper, we present an analysis of the geometric and electronic structures of anisole (PhOMe, Me = CH$_3$) and thioanisole (PhSMe) which are precursors of PPO and PPS, respectively, of some *p*- and *o*-cyano derivatives (*p*-NCPhXMe and *o*-NCPhXR, X = O, R = Me; X = S, R = H, Me, and *t*-But) and of benzonitrile, NCPh, for comparison purposes (see Chart 1 which includes the atom numbering). The acceptor group CN, not present in the polymers, has been introduced in the precursors to mimic the effect of positive charges created by the doping process. The aim of the work is to characterize the electronic structures of the precursors of PPO and PPS and, therefore, to predict which polymer is expected to display better conductivity properties when doped under mild conditions. The ortho-substituted benzonitriles have also been analyzed to gain a deeper insight into the modifications of the geometric and

* To whom correspondence should be addressed. Fax: ++39-0532-240709. E-mail: dsg@dns.unife.it.

10.1021/jp000392w CCC: $19.00 © 2000 American Chemical Society
Published on Web 08/10/2000

CHART 1

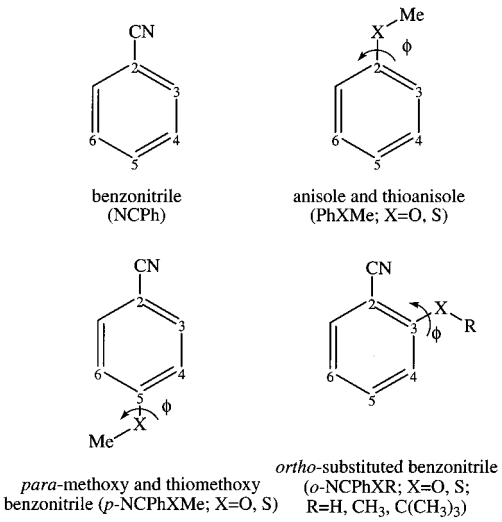

electronic structures brought about by the substitution of sulfur for oxygen in precursors of potentially conducting polymers.

The geometric parameters and the molecular orbital (MO) properties are computed for the neutral and some cation species at the HF/6-31G** level. The energies calculated for the filled and empty MOs are compared with the ionization energy (IE) and electron attachment energy (AE) values measured in the UP and ET spectra, respectively.

The use of Koopmans' theorem (KT) is a good approximation for $\pi-$IE values, while more sophisticated approaches are needed to reproduce AE values. Nevertheless, virtual orbital eigenvalues determined with HF/6-31G*[28] and 6-31G**[29−31] calculations were found to correctly parallel the AE trends, if not their absolute values, when measured in homologous series of π-systems. Here, we verify whether this simple approach is able to account for the ordering and energy variations of the π^* resonances also in the present benzene derivatives, where the assignment of the spectral features to the corresponding MOs is unambiguous.

Experimental Section

UP Spectra. The He(I) spectra were recorded on a Perkin-Elmer PS-18 photoelectron spectrometer connected to a Datalab DL4000 signal analysis system. The bands, calibrated against rare-gas lines, were located using the position of their maxima, which were taken as corresponding to the vertical IE values. The accuracy of the IE values was estimated to be 0.05 eV for peak maxima and 0.1 eV for shoulders. The assignment of PE spectra is based on the composite-molecule approach and the substituent effect, using as reference compounds anisole (PhOMe), thioanisole (PhSMe), and benzonitrile (PhCN).

ET Spectra. Our electron transmission apparatus is in the format devised by Sanche and Schulz[32] and has been previously described.[33] To enhance the visibility of the sharp resonance structures, the impact energy of the electron beam is modulated with a small ac voltage, and the derivative of the electron current transmitted through the gas sample is measured directly by a synchronous lock-in amplifier. The present spectra have been obtained by using the apparatus in the "high-rejection" mode [34] unless otherwise stated, and are therefore related to the nearly total scattering cross section. The midpoint between the maximum and minimum of the derivatized signal has been taken as the most probable, or vertical, AE value. The electron beam resolution was about 50 meV (fwhm). The energy scales were calibrated with reference to the $(1s^12s^2)^2S$ anion state of He. The estimated accuracy is ±0.05 or ±0.1 eV, depending on the number of decimal digits reported.

Calculations. The conformation, bond angles and distances, the Mulliken charge at various atoms and groups, and the molecular orbital energies and localization properties have been computed at the HF/6-31G** level using the Gaussian 94 series of programs[35] for the compounds listed in the Introduction and for benzene and the XMe_2 derivatives. The dependence of the energy upon the angle (ϕ) of rotation of the XMe group around the $C_{ring}-X$ bond for PhXMe and *p*-NCPhXMe has been investigated at intervals of 30° between $\phi = 0°$ (planar conformer with the $C_{ring}-X$ bond in the phenyl ring plane) and $\phi = 90°$ (perpendicular conformer) and at some further ϕ values to better define the potential energy curve close to $\phi = 0°$ (PhSMe) and $\phi = 90°$ (*p*-NCPhOMe). In the analysis of the less symmetric ortho-derivatives the ϕ value ranged from 0° to 180°. All the internal parameters were allowed to relax independently, including the ϕ value at the energy minima. The vertical ionization energy values related to the HOMO of the planar (X = O, S) and perpendicular (X = S) rotamers of PhXMe and *p*-NCPhXMe were computed with the ΔSCF procedure at the UHF level. In the attempt to closely reproduce the conformational properties indicated by the spectroscopic results, the total energy vs ϕ curve for PhSMe has also been computed at the MP2/6-31G**//6-31G** level. Similarly, the geometry of benzonitrile, for which electron diffraction data are available, has been computed at the same level.

Results and Discussion

The UP spectra of *o*-NCPhSR (R = H, Me, *t*-But), *o*-NCPhOMe, and *p*-NCPhXMe (X = O and S) are reported in Figure 1. The ET spectra of *o*- and *p*-NCPhXMe are presented in Figure 2. The IE values lower than about 11.5 eV and the AE values obtained from these spectra are listed in Table 1 together with those of the reference compounds,[33,36−45] the corresponding HF/6-31G** energy levels and the assignments.

The HF/6-31G** relative energies at selected ϕ values for PhXMe, *p*- and *o*-NCPhXMe, and *o*-NCPhXR (R = H and $C(CH_3)_3$) are listed in Table 2, together with the relative abundance of the secondary rotamers with respect to the most stable ones. The torsional potential curves as a function of ϕ (see Chart 1) are plotted in Figures 3, 4, and 7. These curves have been obtained by cubic spline interpolation. The experimental and computed IE and AE values are also presented in the partial energy level diagrams of Figures 5 and 6, respectively. The HF/6-31G** Mulliken charges (e) at the XMe, Ph, and NC groups for the most stable conformer of the monosubstituted benzenes and of para and ortho methoxy and methylthiobenzonitriles are listed in Table 3.

Anisole and Thioanisole. The first three bands of the UP spectrum of PhOMe have been ascribed[39] to ionization from the MOs deriving from the interaction between the $\pi(e_{1g})$ benzene HOMO and the oxygen lone pair orbital perpendicular to the ring plane, O_{lp}. The symmetric component (π_s) of the former is destabilized to 0.8 eV higher energy with respect to the antisymmetric component (π_a), which (essentially) does not interact for overlap reasons.The heteroatom lone pair orbital lying in the ring plane, O_{lpll}, is responsible for the fourth band. Only the planar rotamer ($\phi = 0°$), stabilized by the two electron $\pi^* \leftarrow O_{lp}$ interaction, has been observed in the spectrum in accordance with the small population (about 9%) computed for the gauche rotamer (see below). An estimate of the strength of the $\pi^* \leftarrow O_{lp}$ interaction is provided by the destabilization (0.50

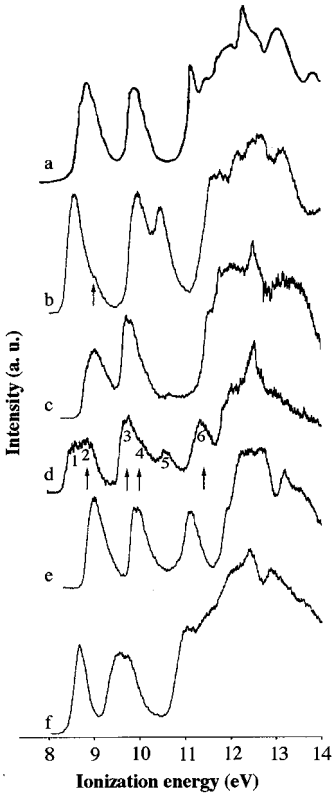

Figure 1. He I photoelectron spectra of substituted benzonitriles (a) *p*-NCPhOMe, (b) *p*-NCPhSMe, (c) *o*-NCPhOMe, (d) *o*-NCPhSMe, (e) *o*-NCPhSH, and (f) *p*-NCPhSC$(CH_3)_3$. The arrows in the spectra of *o*- and *p*-NCPhSMe show the contributions to ionization from the gauche rotamer (see text for discussion of numbers in spectrum d).

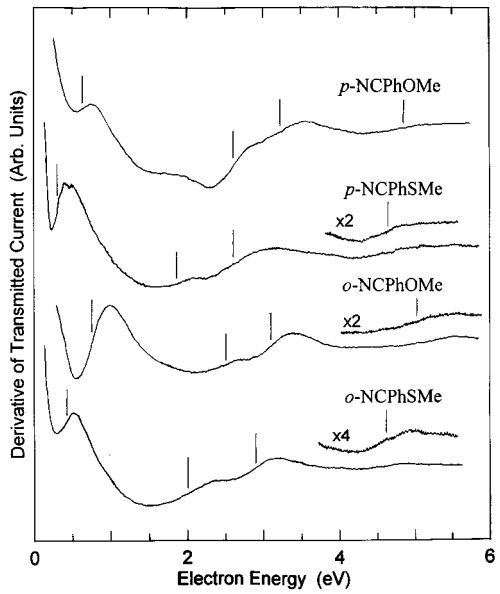

Figure 2. Derivative of the electron current transmitted through *o*- and *p*-NCPhXMe, X = O, S, as a function of the incident electron energy. Vertical lines locate the most probable AEs.

eV) of the empty π_s* MO with respect to the π_a* MO, as evaluated from the ET spectrum of anisole.[45] This energy separation is quantitatively reproduced by the present calculations (Table 1).

The complex band system in the UP spectrum of PhSMe has been ascribed[36,46] to the presence of two rotamers, the planar one having a higher abundance than the gauche one. The higher abundance of the planar conformer is confirmed by the ET

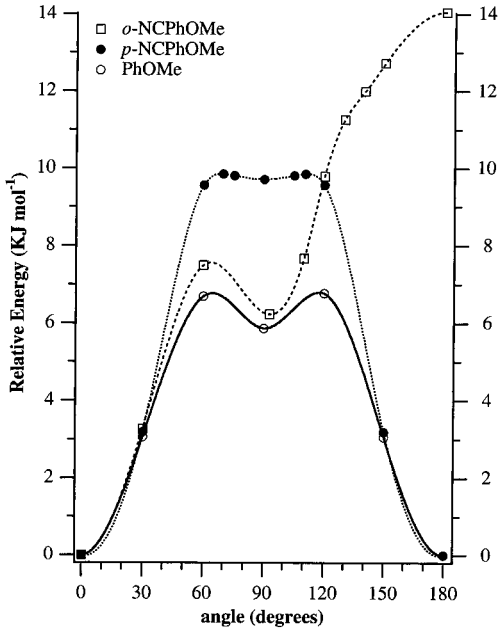

Figure 3. Total SCF ab initio 6-31G** energy vs the substituent torsion angle (ϕ) of *p*-methoxybenzonitrile (filled circles), *o*-methoxybenzonitrile (squares), and anisole (open circles).

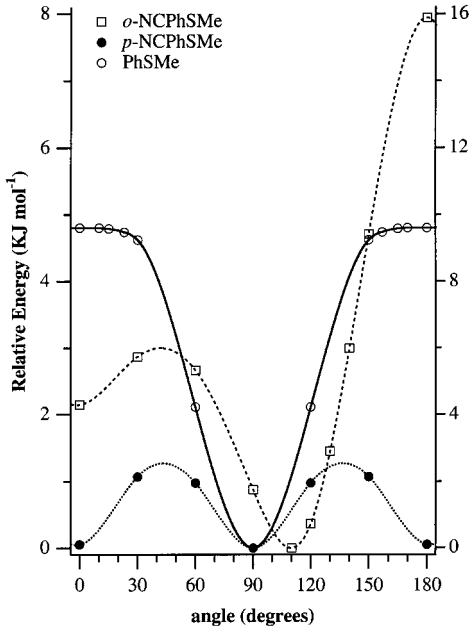

Figure 4. Total SCF ab initio 6-31G** energies vs substituent torsion angles (ϕ) of *p*-methylthiobenzonitrile (closed circles), *o*-methylthiobenzonitrile (squares), and thioanisole (open circles). The right-hand scale refers to *o*-NCPhMe.

spectrum of thioanisole, which differs from that of its (rotated) 2,6-dimethyl derivative.[47] The presence of a rotated conformer in thioanisole, but not in anisole, could be due to (i) an S_{3p}/π* overlap lower than the O_{2p}/π* overlap in the planar conformer or (ii) the occurrence of σ^*_{S-C}/π mixing in the perpendicular conformer of thioanisole, the corresponding interaction being less important in anisole owing to the high energy of the σ^*_{O-C} MO.

The energies calculated for the filled MOs closely reproduce the IEs (see Table 1), except for the O_{2p} and (to a lesser extent) the S_{3p} MOs due to the strong relaxation energy associated with electron removal from a contracted heteroatom atomic orbital, as previously observed.[15,29] Although an accurate evaluation of

TABLE 1: Experimental IE and AE Values (eV) for Benzene, XMe_2, NCPh, the Planar and Gauche (in Parentheses) Conformers of PhXMe, *p*-NCPhXMe, *o*- NCPhXMe (X = O and S), and *o*-NCPhSR (R = H and $C(CH_3)_3$), and Corresponding Data Computed at the HF-Koopmans (KT) and HF-ΔSCF Level Using the 6-31G Basis Set**

	filled MOs				empty MOs		
	expt	assignment	KT	ΔSCF	expt	assignment	KT
benzene	9.24[38]	π_s, π_a	−9.0		4.82[33]	π_o*	10.05
	12.15	πo	−13.55		1.12	π_s*,π_a*	4.06
MeOMe	10.04[40]	O_{lp}	−11.34		6.0[44]	σ_{OMe}*	8.11
	11.91	$O_{lp\|\|}$	−12.90				
	13.43	σ_{OMe}	−14.38				
MeSMe	8.72[38]	S_{lp}	−9.08		3.25[41]	σ_{SMe}*	5.36
	11.47	$S_{lp\|\|}$	−11.74				
	12.68	σ_{SMe}	−13.49				
PhOMe	8.42[39]	π_s	−8.30 (−8.76)	7.05 (8.93)	4.85[45]	π_o*	10.36 (10.37)
$\phi = 0°$ ($\phi = 90°$)	9.23	πa	−9.11 (−9.13)		1.65	π_s*	4.51 (4.19)
	11.02	O_{lp}	−12.58 (−11.83)		1.13	π_a*	3.99bh47arani(3.93)
	11.5	$O_{lp\|\|}$	−12.91 (−13.15)				
PhSMe	8.02[36] (8.55)	S_{lp}	−8.02 (−9.31)	6.83 (7.57)	4.45[45]	π_o*	9.75 (10.01)
$\phi = 0°$ ($\phi = 90°$)	9.25 (9.25)	π_a	−9.20 (−9.21)		2.7	σ_{SMe}*	5.24 (5.66)
	10.20 (9.25)	π_s	−12.0 (−9.10)		0.9	π_s*	3.92 (3.40)
	11.12 (11.10)	$S_{lp\|\|}$	−10.76 (−11.99)		0.9	π_a*	3.86 (3.82)
NCPh	9.71[42]	πs	−9.66		4.8	π_o*	10.−19
	10.17	πa	−9.84		3.21	$\pi_{CN\perp}$*	7.32
	12.24	$\pi_{CN\|\|}$	−12.75		2.53	$\pi_{CN\|\|}$*	5.99
	13.09	$\pi_{CN\perp}$	−13.09		0.55	π_a*	3.28
					−0.24[43]	π_s*	2.44
p-NCPhOMe	8.92[37]	πs	−8.93 (−9.38)	7.58 (9.48)	4.9	π_o*	10.44 (10.34)
$\phi = 0°$ ($\phi = 90°$)	9.97	π_a	−9.94 (−9.95)		3.3	$\pi_{CN\perp}$*	7.58 (1.27)
	11.3	O_{lp}	−13.7 (−12.46)		2.65	$\pi_{CN\|\|}$*	6.12 (6.02)
		$\pi_{CN\perp}$	−12.5 (−12.89)		0.66	π_a*	3.28 (3.19)
		$\pi_{CN\|\|}$	−12.6 (−12.73)			π_s*	2.85 (2.19)
p-NCPhSMe	8.56 (8.96)	S_{lp}	−8.62 (−9.81)	7.28 (8.03)	4.63	π_o*	10.07 (10.01)
$\phi = 0°$ ($\phi = 90°$)	9.86	π_a	−10.00 (−10.01)		2.63	$\pi_{CN\perp}$*	7.15 (6.80)
	10.46	π_s	−11.17 (−9.69)		1.87	$\pi_{CN\|\|}$*	6.04 (5.87)
	11.8	$S_{lp\|\|}$	−12.60 (−12.41)			σ_{SMe}*	4.74 (5.06)
					0.30	π_a*	3.17 (3.10)
						π_s*	2.38 (2.00)
o-NCPhOMe	9.0	π_s[b]	−8.97 (−9.43)		5.1	π_o*	10.79 (10.55)
$\phi = 0°$ ($\phi = 92.9°$)	9.75	π_a[b]	−9.73 (−9.76)		3.13	$\pi_{CN\perp}$*	7.40 (7.37)
	11.55	O_{lp}	−13.51 (−12.40)		2.53	$\pi_{CN\|\|}$*	6.11[a] (6.04[c])
	12.0	$\pi_{CN\|\|}$	−12.46 (−12.73)		0.77	π_a*[e]	3.76 (3.44)
		$\pi_{CN\perp}$	−12.85 (−13.04)			π_s*[e]	2.56 (2.46)
o-NCPhSMe	8.58 (8.8)	S_{lp}	−8.62 (−9.33)		4.7	π_o*	10.18 (10.22)
$\phi = 0°$ ($\phi = 110.1°$)	9.73 (9.73)	π_a[b]	−9.77 (−9.80)		2.92	$\pi_{CN\perp}$*	7.14 (7.16)
	10.68 (10.1)	π_s[b]	−11.33 (−10.17)		2.0	$\pi_{CN\|\|}$*	6.30 (5.90)[d]
	11.43 (11.43)	$\pi_{CN\|\|}$ (-S_{lp})	−12.23 (−12.40)			σ_{SMe}*	4.75 (5.20)
		$CN_{\|\|}$ (+$S_{lp\|\|}$)	−12.97 (−12.89)		0.45	π_a*[e]	3.26 (2.98)
		$\pi_{CN\perp}$	−13.09 (−13.20)			π_s*[e]	2.38 (2.15)
o-NCPhSH	8.95	πs	−8.94 (−8.93)			π_o*	10.12
$\phi = 0°$ ($\phi = 180°$)	9.91	πa	−9.89 (−9.92)			$\pi_{CN\perp}$*	7.13
	11.1	S_{lp}	−11.81 (−11.80)			$\pi_{CN\|\|}$* + σ_{SH}*	5.88[f]
		$\pi_{CN\|\|}$ +σ_{CSH}	−12.66 (−12.98)			σ_{CSH}*	4.11
		π_{CN}z	−13.25 (−13.40)			π_a*[e]	3.11
		σ_{CSH} + $\pi_{CN\|\|}$	−13.46 (−13.32)			π_s*[e]	2.28
o-NCPhSC$(CH_3)_3$	8.70	S_{lp}	−9.50			π_o* + σ_{SC}*	10.19
$\phi = 88.5°$ ($\phi = 180°$)	9.60	π_a	−9.76			$\pi_{CN\perp}$*	7.19
	9.80	π_s	−9.61			$\pi_{CN\|\|}$*	6.09
	11.2	$S_{lp\|\|}$	−11.89			σ_{SC}*	5.34
		$\pi_{CN\|\|}$ +σ_{SC}	−12.74[g]			π_a*[e]	2.95
		$\pi_{CN\perp}$	−13.04			π_s*[e]	2.21

[a] Average value of two MOs of very similar parentage computed at 5.92 and 6.31 eV. [b] Symmetry referred to the XMe substituent. [c] Average value of two MOs of very similar parentage computed at 5.95 and 6.12 eV. [d] Average value of two MOs of very similar parentage computed at 5.92 and 6.31 eV. [e] Symmetry referred to the NC substituent. [f] Average value of two MOs of very similar parentage computed at 5.61 and 6.14 eV. [g] Average value of two MOs of very similar parentage computed at 12.60 and 12.88 eV.

anion state energies is beyond the limits of the HF/6-31G** calculations, the experimental AE trends are also nicely reproduced, as previously found in other series of homologous compounds.[28−31] In particular, the calculations predict the energy ordering π_s* above π_a* in PhOMe, the near degeneracy of these two MOs and the presence of a low-energy σ* MO in PhSMe, and the reverse ordering (π_s* below π_a*) in the rotated conformer of PhSMe, in agreement with experiment.[47]

The PhOMe torsional potential curve (Figure 3) has two minima corresponding to the planar and to the less populated perpendicular conformer. The latter is less stable by 5.82 kJ/mol, and the activation energy to go from the planar to the perpendicular conformer is about 6.77 kJ/mol. The calculations, however, are unable to correctly predict the relative stability of the two rotamers for PhSMe (see Table 2 and Figure 4), as previously found for 3-methylthiothiophene.[13] In particular, the HF calculations predict only one minimum at $\phi = 90°$. The regions $0° < \phi < 30°$ and $150° < \phi < 180°$ are rather flat and the curve rises monotonically and reaches a maximum at $\phi = 0°$ ($\phi = 180°$) where the energy is 4.84 kJ/mol higher than that of the perpendicular conformer. The analysis of the vibrational frequencies confirms that the planar conformer is a first order

TABLE 2: Relative HF/6-31G Energies (kJ/mol) at Different Torsional Angles (ϕ, deg) and Relative Abundance (in Parentheses) of the Secondary Minima with Respect to the Most Stable Ones Calculated for PhXMe, *p*-NCPhXMe, O-NCPhXMe, and O-NCPhSR (R = H, C(CH$_3$)$_3$), and (in Italics) Relative MP2/6-31G** Energies for Various Rotamers of PhXMe (X = O, S)**

	PhXMe		*p*-NCPhXMe		*o*-NCPhXMe		*o*-NCPhSR	
ϕ	X = O	X = S	X = O	X = S	X = O	X = S	R = H	R = *t*-But
0	0.0[a] (100%)	4.81[a,c]	0.0[a] (100%)	0.05[a] (98.0%)	0.0[a] (100%)	4.29[a] (18.1%)	5.02[a] (13.5%)	21.93
		2.23						
15		4.79						
30	3.06	4.71	3.19	1.07	3.27	5.74	6.55	19.43
		1.66						
43.12				1.27[b]				
42.6						6.0[b]		
60	6.69	2.18	9.56	0.98	7.50	5.33	8.14	9.76
		0.34						
61.7							8.15[b]	
64.1					7.56[b]			
64.97	6.77[b]							
69.50			9.85[b]					
75			9.81					
88.5								0.0[a]
90	5.87[a] (9.6%)	0.0[a]	9.71[a] (2.1%)	0.0[a] (100%)		1.76	6.82	0.04
		0.0						
92.86					6.23[a] (8.3%)			
110.11						0.0[a] (100%)		
120					9.78	0.72	3.86	17.64
150					12.73	9.42	1.12	34.09
180					14.04[c]	15.89[c]	0.0[a] (100%)	43.30[c]

[a] Optimized ϕ value. [b] Interpolated value from the fitting curve. [c] Saddle point.

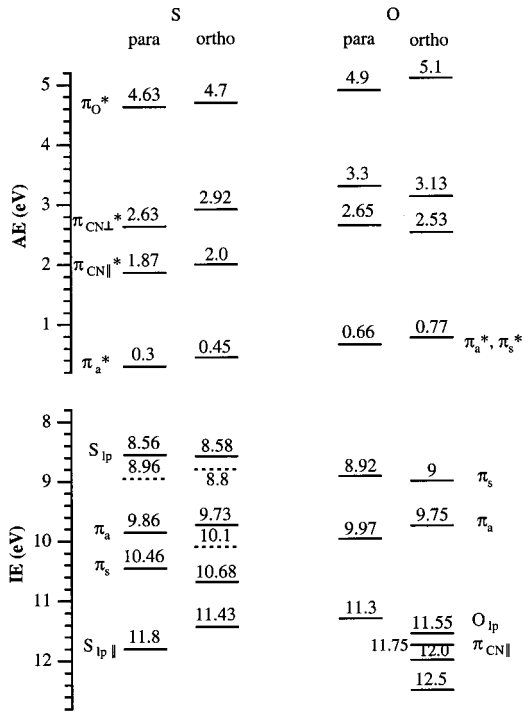

Figure 5. Partial energy level diagram for filled and empty MOs obtained by UP and ET spectroscopies for *o*- and *p*-methoxy- and methylthiobenzonitriles.

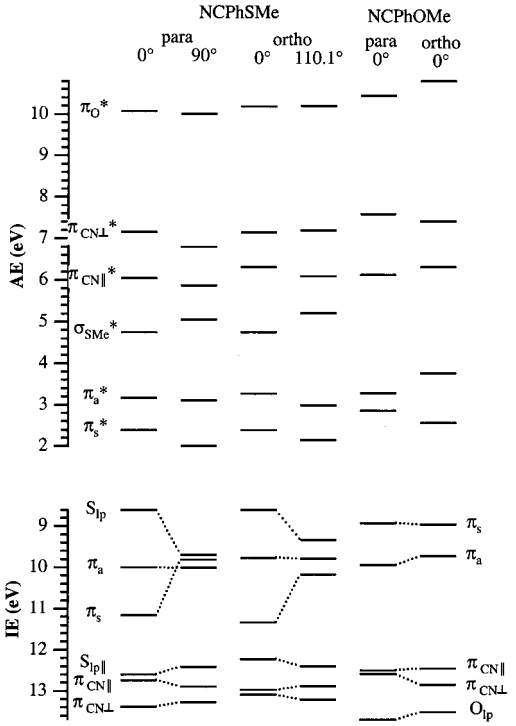

Figure 6. Theoretical (HF/6-31G**) energy level correlation diagrams for the most stable rotamers of *o*- and *p*-methoxy- and methylthiobenzonitriles.

saddle point on the energy hypersurface. The torsional potential curve obtained at the MP2/6-31G**//6-31G** level is similar to that obtained by HF calculations, although the maxima are only 2.23 kJ/mol above the perpendicular minimum. The relative energies at selected ϕ values are reported in italics in Table 2. The inclusion of electron energy correlation lowers the barrier to rotation of the SMe group, but the maximum at $\phi = 0°$ remains.

In order to investigate the origin of the high energy predicted for the planar conformer of thionisole, we have analyzed the geometry and the Mulliken charge distributions of the present compounds. The geometries of benzonitrile,[48] benzene,[49] and anisole[50] determined by electron diffraction measurements are reproduced with good accuracy by the HF/6-31G** calculations. In particular, the substituted molecules are almost perfectly planar, with the bond angles and lengths close to the standard values for benzene and the C−C−N and C−O−C angles equal to 180.0° and 119.8° for benzonitrile and anisole, respectively.

Thus, the HF/6-31G** calculations appear to be appropriate for the description of the geometry of the present disubstituted

TABLE 3: Computed (HF/6-31G) Mulliken Charges (e) at Selected Groups for NCPh and the Most Stable Conformers of PhXMe and *p*- and *o*-NCPhXMe (X = O, S)**

			NCPhOMe			NCPhSMe	
	NCPh	PhOMe	para	ortho	PhSMe	para	ortho
ϕ		0°	0°	0°	90°	90°	110.1°
XMe		−0.325	−0.301	−0.298	0.104	0.134	0.172
Ph	0.183	0.325	0.493	0.448	−0.104	0.043	0.004
NC	−0.183		−0.192	−0.150		−0.177	−0.176

molecules for which, to our knowledge, the geometry has not been experimentally determined. According to the calculations, the presence of the *p*-XMe group does not significantly modify the geometry with respect to benzonitrile: the ring C−C bond lengths being 1.387 ± 0.014 Å and the bond angles = 119.96 ± 1.26°. On going from the rotated to the planar conformers the value of the C−X−C bond angle increases by ca. 4°, and the C_{ring}−X bond deviate from the bisectrix of the ring angle of the carbon atom by ∼ 4° to relieve in part the steric hindrance between the methyl group and the facing CH group of the ring.

The contacts between the atoms of the CH and CH_3 groups are slightly shorter than the sum of the corresponding van der Waals radii[51] in both anisole and thioanisole. A significant difference is observed in the charge at the C atom of the Me group, which is quite high (ca. −0.5 e) when X = S and nearly zero when X = O. This gives an electrostatic repulsion with the negatively charged C(ring) (ca. −0.2 e in all cases) 1 order of magnitude larger in the sulfur derivative. An overestimation of this interaction could be responsible for the failure of the calculations in predicting an energy minimum for ϕ=0°.

***p*-Methylthio and *p*-Methoxybenzonitrile**. The assignments of the UP and ET spectra of *p*-NCPhXMe are based on those of the reference molecules PhXMe and NCPh and are shown in Figures 5 and 6. For the sake of consistency, we reran the ET spectrum of benzonitrile. The measured AE values (reported in Table 1) are very close to those previously found.[52] The analysis of the UP[42] and ET spectra and of the first electron affinity value[43] of benzonitrile can be summarized as follows (see Table 1). Mixing between the filled π_s and empty π_s* ring orbitals of benzene with the cyano group π-orbitals perpendicular to the ring plane ($\pi_{CN\perp}$ and $\pi_{CN\perp}$*) causes the stabilization of the $\pi_{CN\perp}$ (0.85 eV) and of the π_s* (0.3 eV) MOs and the destabilization of the π_s (0.46 eV) and of the $\pi_{CN\perp}$* (0.68 eV) MOs with respect to the appropriate antisymmetric π-ring orbitals (π_a,π_a*) or π-cyano orbitals lying in the ring plane ($\pi_{CN\parallel}$, $\pi_{CN\parallel}$*). In particular, the first anion state (associated with the π_s* MO) of NCPh is 0.24 eV[43] more stable than the neutral molecule and cannot thus be detected in ETS. The electron-withdrawing effect of the cyano group stabilizes the noninteracting filled π_a and empty π_a* MOs by about 0.7 eV with respect to the corresponding benzene orbitals.

The low IE region (IE <11.5 eV) of the UP spectrum of *p*-NCPhOMe[37] and *p*-NCPhSMe (Figure 1) shows three bands which, on the basis of eigenvector analysis and comparison with the IE values of the reference compounds NCPh and XMe_2, can be ascribed to ionization from the MOs of mainly π_s, π_a, and X_{lp} origin (see Table 1). The comparison of the energy difference between the first and the third band of the *p*-NCPhOMe spectrum with the computed data for the planar and gauche rotamers indicates that the spectral features derive from the planar rotamer. In agreement with this, the HF/6-31G** potential energy curve as a function of ϕ (see Figure 3 and Table 2) has two minima corresponding to the planar and perpendicular conformers but the latter is very shallow and less stable by 9.77 kJ/mol. If the potential energy curves for PhOMe and *p*-NCPhOMe are normalized at their maxima (ϕ ca. 60° and 120°, see Figure 3) where the stabilizing two-electron interactions of the stable rotamers are minimized, it can be observed that the introduction of the *p*-NC group stabilizes the planar rotamer but destabilizes the gauche one with respect to the corresponding minima of the unsubstituted rotamers. In particular, the relative population of the perpendicular conformer decreases from 9.6 to 2.1% with respect to the planar one (see Table 2). The stabilization of the planar rotamer is in agreement with the stabilization of the π_s* orbital on going from benzene (1.12 eV[33]) to NC−Ph (−0.24 eV[43]) which favors the π_s* ← O_{lp} CT interaction.

The ET spectrum of *p*-NCPhOMe (see Figure 3) shows four resonances, slightly higher in energy (ca. 0.1 eV) with respect to the corresponding signals in NCPh (see Table 1). *p*-OMe substitution is expected to perturb mainly the benzonitrile π_s* LUMO, due to mixing with the O_{lp} orbital. The destabilization of the benzonitrile LUMO, however, should be smaller than that (0.51 eV) observed on going from benzene to anisole, due to its smaller localization at the benzene ring. The π_s* resonance should thus lie in the 0−0.2 eV energy range, where it is hidden by the intense electron beam signal. Consistently, the calculations predict the π_s* MO to be 0.43 eV lower in energy than the π_a* MO (AE = 0.66 eV) and the width of the first observed resonance is no larger than that of the corresponding resonance in NCPh, indicating that also in NCPhOMe this signal is due only to the π_a* MO.

The first band in the UP spectrum of *p*-NCPhSMe (IE = 8.56 eV, Figure 1b) shows a weak shoulder on the high energy side (ΔIE ∼ 0.4 eV) which, by comparison with the spectrum of PhSMe (ΔIE ∼ 0.5 eV[36]) and the calculations (see Figures 5 and 6), can be ascribed to a rotamer with a less effective S_{lp}−π(ring) conjugation whose population (as deduced from the UP spectrum) is ≤25% of that of the prevailing planar rotamer. As observed for PhSMe and 3-methylthiothiophene,[13] once again the calculations overestimate the stability of the gauche rotamer which is predicted to be nearly as abundant as the planar one (see Table 2).

The four resonances present in the ET spectrum of *p*-NCPhSMe are lower in energy (0.1−0.3 eV) with respect to those of the corresponding oxy derivative. In contrast to the OCH_3 group, the SCH_3 group leads to a stabilization of the π_s* MO.[45,47,53] The first anion state of NCPhSMe is thus expected to be significantly more stable than that of the oxy derivative and even more stable than that of NCPh, in line with the calculated LUMO energies (Table 1). The first resonance displayed in the ET spectrum (0.30 eV) is therefore associated with the π_a* MO. Its energy is lower than that of the corresponding resonance in NCPh and NCPhOMe. In agreement, the ET spectrum of *p*-dimethylthiobenzene[53] showed that thio substitution stabilizes the π_a* resonance, although to a lesser extent with respect to the π_s* resonance. The two features centered at 1.87 and 2.63 eV are associated with electron capture into the $\pi_{CN\parallel}$ and $\pi_{CN\parallel}$* MOs. In this energy region, however, a σ_{S-C}* resonance (2.70 eV in thioanisole[45,47]) is also expected. The weaker σ* signal is probably hidden by the $\pi_{CN\perp}$* signal. The NC group stabilizes the filled and empty MOs with respect to the corresponding orbitals of PhSMe (see Table 1).

The stabilization of the planar rotamer relative to PhSMe is consistent with the stabilization of the π_s* MO, which makes the π_s* ← S_{lp} CT interaction easier. The two minima in the calculated torsional potential curve are quasi isoenergetic (ΔE = 0.05 kJ/mol, see Table 2 and Figure 4) and are connected by a low barrier to rotation (1.27 kJ/mol) which would allow nearly

free rotation around the $C_{ring}-S$ bond at room temperature, in contrast with the spectroscopic observations.

Electronic Structure and Electric Conductivity. Electric conductivity occurs via migration, under an applied electric field, of charge defects localized along the polymer chain.[5,9] Therefore, conductivity depends inter alia upon the molecular polarizability. The smaller π_s-IE and π_s^*-AE values of the sulfur derivatives PhSMe and *p*-NCPhSMe with respect to the corresponding methoxy derivatives suggest that PPS has a smaller HOMO−LUMO energy gap than PPO and a better possibility to give rise to materials with high electric conductivity when properly doped as, in fact, observed for low doping levels.[26,27]

The electron relaxation energy (E_{relax}) accompanying positive ionization can be taken as an independent estimate of polarizability. It can be noticed (see Table 1) that the first experimental IE value for the $\phi = 0°$ rotamer of PhXMe and *p*-NCPhXMe is reproduced within 0.12 eV by the HF/6-31G** calculations at the Koopmans' theorem level. E_{relax} and the change in correlation energy (ΔE_{corr}) associated with the removal of the outermost electron, therefore, nearly exactly compensate each other. On the other hand, the first IE value for the gauche rotamer of PhSMe and *p*-NCPhSMe is computed to be too high by 0.9 eV at the KT level. This discrepancy, already observed for heteroatom lone pair orbitals,[13,29,54] is ascribed to the larger electron relaxation accompanying ionization from a localized AO (X lone pair) compared to a delocalized π_s MO.

E_{relax} for a valence ionization can be evaluated as the difference between the computed KT value (which neglects both E_{relax} and ΔE_{corr}) and the vertical IE value obtained from the neutral-cation ΔSCF procedure (which takes into account E_{relax}). The data of Table 1 indicate that E_{relax} is nearly constant (1.19−1.35 eV) for the planar rotamer of PhXMe and *p*-NCPhXMe. However, when the system is more strongly perturbed, the thio group shows a larger capability to relax. This has been observed in the X-ray photoelectron spectra of *p*-NO_2-PhXMe (with X = O[55] and S[56]), where core ionization at the nitro group produces intense shake-up peaks (due to many-electron processes) involving charge-transfer (CT) interaction from the donor to the acceptor group. These signals are more intense and closer in energy to the main peak in the thio derivative, in agreement with its greater polarizability. Recalling that electric conductivity in p-doped polymers occurs via positive charges (bipolarons) drifting under the applied electric field,[5,9] the above-reported properties of the thio derivatives are in line with their greater ability to carry electricity along the polymer chain.

Ortho Derivatives. The variation of the potential energy function of *o*-NCPhOMe with respect to the dihedral angle ϕ (Figure 3) shows two minima associated with a planar ($\phi = 0°$) and a shallow gauche ($\phi = 92.8°$) rotamer, the latter being less stable by 6.23 kJ/mol. Two minima are also present in the *o*-NCPhSMe torsional potential curve (Figure 4) but, in this case, the $\phi = 110.11°$ gauche conformer is 4.29 kJ/mol more stable than the shallow $\phi = 0°$ planar one. The steric hindrance between the two substituents renders unstable the $\phi = 180°$ planar rotamer for both compounds. Additional information on the torsional potential curves is available from Table 2.

The most stable ortho isomer is 6.91 (X = O) or 6.35 (X = S) kJ/mol less stable than the corresponding para one owing to partial compensation of opposite effects. Steric hindrance between the two substituents, indicated by X- - -C_{CN} contacts (2.71 (X = O) and 3.19 (X = S) Å) shorter than the sum of the corresponding van der Waals radii (3.22 and 3.50 Å,[51] respectively) and by the enlargement (ca. 2°) of the SC(2)C(3) and C(2)C(3)C_{CN} angles in the gauche rotamer of *o*-NCPhSMe, causes an increase in the total energy. The electrostatic interaction between the X and C_{CN} atoms (q(O) = −0.658 e, q(C_{CN}) = 0.310 e; q(S) = 0.189 e; q(C_{CN}) = 0.289 e) gives a stabilizing contribution to the total energy in *o*-NCPhOMe while it is repulsive in the sulfur compound. Finally, the stabilizing two-electron interaction is reduced in the ortho compounds more for X = O than for X = S because it is stronger in the corresponding para oxy derivative.

The UP spectrum of *o*-NCPhOMe (see Figure 1) shows three peaks in the low IE (<11.5 eV) region ascribed to ionization from the π_s, π_a, and O_{lp} MOs of the planar rotamer by comparison with the spectra of related compounds and in agreement with eigenvector analysis. The symmetry symbols π_s and π_a refer to the OMe substituent which dominates over the NC substituent in determining the nodal properties of the ring MOs. In the corresponding thio derivative, the effect of the SMe group dominates for the filled MOs, while the NC group prevails for the empty orbitals. As usual,[40] the bands in the UP spectra of the oxygen derivatives are broader than those of the corresponding thio compounds. However, the absence of clear shoulders in the spectrum of *o*-NCPhOMe indicates an upper limit of 10% relative intensity for the gauche rotamer with respect to that of the main rotamer, in agreement with the results of the calculations (8.3%, see Table 2 and Figure 1, where the low-intensity signal at about 10.5 eV is likely due to an impurity).

Six bands are present in the low IE region of the UP spectrum of *o*-NCPhSMe: four of similar intensity and two (the third and the sixth) of nearly double intensity. A comparison of the experimental IE values with the computed data for the planar and gauche rotamer and with the corresponding data for the para derivative (see Figure 6) indicates that the spectrum derives from the simultaneous presence of the two most stable conformers. In particular, the planar (anti) conformer with large π_{ring}/S_{lp} interaction contributes to the bands labeled 1, 3, 5, and 6 in Figure 1, while the gauche conformer generates bands numbered 2, 3, 4, and 6. Bands 1 and 2 have nearly equal intensity, indicating that the two conformers are of similar abundance, assuming equal ionization cross sections. This experimental finding appears to be in conflict with the HF/6-31G** results, according to which the intensity of the planar rotamer is only 18.1% of that of the gauche ($\phi = 110.11°$) one. The overestimation of the gauche rotamer stability by the calculations is in line with the above results for *p*-NCPhSMe and PhSMe and with those previously reported[13] for 3-methylthiothiophene at the HF and MP2 levels and is, therefore, not related to the direct through-space interaction between the two substituents in *o*-NCPhSMe.

The ET spectra of both the *o*-NCPhXMe compounds show four resonances ascribed to MOs mainly localized at the ring or at the NC group by analogy with the previously discussed benzonitriles and in agreement with the results of the calculations (see Table 1 and Figures 5 and 6). In the ET spectrum of *o*-NCPhOMe the resonances associated with MOs mainly localized at the ring (π_a^*, π_s^*, and π_o^*) are slightly (0.1−0.2 eV) destabilized, while those associated with the CN group ($\pi_{CN\parallel}^*$ and $\pi_{CN\perp}^*$) are stabilized by a similar amount with respect to the para-substituted compound (see Figure 5) in agreement with the calculated energy levels reported in Table 1. The resonances displayed by the spectrum of *o*-NCPhSMe are slightly (0.1−0.3 eV) destabilized with respect to the corresponding resonances in the para derivative, mainly those related to the π_{CN}^* MOs. This trend is present, although less pronounced, in the computed orbital energies. The energy shifts

in the AE values parallel the charge density variations predicted by the calculations on changing the substituents and their relative orientations. Table 3 collects the Mulliken charges (e) at the CN, Ph, and XMe groups of the mono- and disubstituted benzenes. The analysis of these data indicates that on going from PhOMe and NCPh to *p*-NCPhOMe the electron density increases at the Ph and CN groups with a corresponding loss at the OMe group, in line with the occurrence of the above-mentioned $\pi^* \leftarrow O_{lp}$ CT interaction. In the ortho isomer, the charge at the OMe group does not change significantly with respect to the para derivative, but the ring is less effective in transferring the charge at the CN group. Thus, the CN and the Ph groups have a less negative and a less positive charge density, respectively, with respect to the para derivative, in agreement with the observed AE shifts.

At variance with the methoxy analogues, in *o*-NCPhSMe the charge at the CN group does not decrease with respect to *p*-NCPhSMe. This fact and the concomitant destabilization of the π_{CN}^* MOs in *o*-NCPhSMe could be due to through-space mixing between orbitals of prevailing sulfur and CN character. The eigenvector analysis indicates that this interaction is much larger for the heavier heteroatom, in agreement with the larger size and the more propitious energy gap between the interacting orbitals. These interactions, however, do not appear to influence the computed CN bond distance (1.1365 ± 0.0005 Å) which does not change with the nature, the ring position or the angle of rotation of the XMe substituent.

There is no direct evidence from the ET spectrum of the thio derivatives for the presence of more than one conformer, while evidence is obtained from the UP spectrum. The HF/6-31G** calculations qualitatively reproduce the increase of the planar rotamer with respect to the gauche one on going from PhSMe to *p*-NCPhSMe, as well as its decrease on going from the para to the ortho derivative. To obtain more information on the capability of the present level of calculations to predict the most stable conformation of thioanisoles, the analysis has been extended to *o*-NCPhSR, R = H and $C(CH_3)_3$. The UP spectra are included in Figure 1, while the dependence of the energy from the angle of rotation of the SR group around the $C_{ring}-S$ bond is shown in Figure 7. The potential energy plot for *o*-NCPhSH has two minima at $\phi = 0°$ (anti rotamer) and 180E (syn rotamer), the former being less stable by 5.02 kJ/mol. The computed energy levels are nearly equal for the two rotamers, except those related to the mixing between the empty and filled orbitals of the NC and SH groups lying in the main molecular plane whose splitting in the anti conformer is 0.3 or 0.4 eV larger, respectively, than in the syn conformer. In agreement, the bands at 8.95 and 11.10 eV derive from electron ejection from the strongly interacting S_{lp} and π_s orbitals, the splitting (2.15 eV) being close to that of the planar *o*-NCPhSMe (2.1 eV), while the band at 9.91 eV is due to ionization from the π_a MO. The lack of the gauche minimum in the SH derivative could be due to the high σ_{SH} value (15.35 eV[40]) compared with the σ_{SMe} value (12.68 eV[38]) which reduces the strength of the CT interaction with the empty π^* ring orbitals.

The H/SH atom is easily accommodated into the syn rotamer, without important geometric variations. In particular, both conformers are perfectly planar and the relevant bond distances and angles of the anti conformer are close to the corresponding values for the SMe derivative, while the $C(3)-C(2)-C_{CN}$, $C(2)-C(3)-S$ and $C(3)-S-H$ bond angles of the syn rotamer are 2°−4° larger than in the anti derivative. The corresponding angles for the *t*-But derivative are similarly increased and, in addition, the two substituents deviate by 3°−5° from the ring plane in the opposite direction and distort and slightly repel each other.

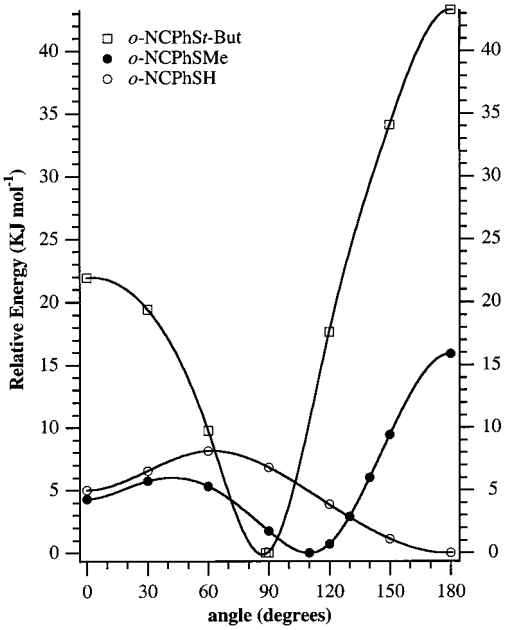

Figure 7. Total SCF ab initio 6-31G** energies vs. the substituent torsion angles (ö) for the ortho-substituted benzonitriles *o*-NCPhSR (R = H, CH_3 and $C(CH_3)_3$).

The splitting (1.1 eV) between the first (S_{lp}) and the third (π_s) band in the spectrum of *o*-$NCPhSC(CH_3)_3$ is close to that (ca. 1.3 eV) of the gauche rotamer of *o*-NCPhSMe and thus only one rotamer (gauche, with $\phi = 88.5°$) is predicted to be stable. The energy rapidly increases for small deviations in the ϕ value from the minimum energy value because of the large steric hindrance of the bulky *t*-butyl substituent (see Figure 7). The calculations, therefore, agree with the spectra predicting only planar and orthogonal conformers for R = H and $C(CH_3)_3$, respectively.

It would thus seem that the ab initio HF/6-31G** and MP2/6-31G** calculations reproduce, with different levels of accuracy, the planar and gauche rotamers of thioanisole, the stability of the former being underestimated. However, the variation of the S_{lp}/π^* interaction due to the introduction of an acceptor ring substituent, as well as the variation of the SR/ring hyperconjugative interaction by changing R from Me to H and $C(CH_3)_3$, are quantitatively reproduced by the HF/6-31G** calculations.

Conclusions

The UP and the ET spectra of *p*-NCPhXMe and *o*-NCPhXMe (X = O and S) and the UP spectra of *o*-NCPhSR (R = H and *t*-But) have been assigned by comparison with the assignment of the spectra of simple related molecules and with the results of HF/6-31G** energy level calculations. Additional information on the preferred gas-phase conformation of the PhXMe and the disubstituted derivatives has been obtained by comparing the UP spectra with the computed potential energy curves as a function of the angle of rotation of the XR substituent. In particular, the oxygen derivatives PhOMe, *p*-NCPhOMe, and *o*-NCPhOMe prefer a planar conformation with the C atom of the Me group lying in the main ring plane ($\phi = 0°$). The planar conformation allows the largest $O_{lp\perp}/\pi$ mesomeric interaction and is stabilized by the $\pi_{ring}^* \leftarrow O_{lp\perp}$ CT interaction. The gauche minimum ($\phi = 90°$), stabilized by the π_{ring}/σ_{OMe} CT interactions, is predicted to be much less populated (2−10%) than the

corresponding planar one, in agreement with the absence of spectral features which could be related to a conformer with reduced π/O_{lp} orbital interaction.

The UP spectrum of the SMe derivatives shows the presence of two (groups of) rotamers, with large or reduced sulfur−ring conjugation. The relative abundance of the rotamers depends upon the number and the relative position of the substituents. The calculations reproduce the experimentally observed increase in the population of the planar rotamer on going from PhSMe to *p*-NCPhSMe as well its decrease on going from the para to the ortho isomer. In all cases, however, the calculations overestimate the stability of the gauche conformer.

PhSMe and *p*-NCPhSMe have a HOMO−LUMO (π_s/π_s^*) energy gap (<9.0 eV) smaller than the corresponding value (>9.5 eV) in the oxy derivatives. In addition, the two rotamers of the thio derivatives have similar energy and their valence energy levels do not differ significantly. PPS is, therefore, more suitable than PPO for incorporating counteranions introduced during the doping process into the crystal lattice. Furthermore, neutral/cation ΔSCF calculations coupled with previous XPS data indicate that the methylthio- group has a larger polarizability than the methoxy- group. These properties agree with the greater capability of the corresponding polymer to carry electrical charge along the molecular chain when properly doped.

Steric hindrance between the two substituents, small geometric deformations, and the reduced strength of the two-electron interactions render the *o*-NCPhXMe derivatives (6.35−6.91 kJ/mol) less stable than the corresponding para ones. Small shifts in the AE values with respect to the para derivatives have been ascribed, with the help of charge density calculations, to through-space CT interaction between the ortho substituents.

Finally, the HF/6-31G** calculations correctly predict, in agreement with the analysis of the UP spectra, that the most stable rotamers of *o*-NCPhSH and *o*-NCPhStBut are, respectively, planar and gauche.

Acknowledgment. The authors thank the Italian Ministero dell'Università e della Ricerca Scientifica e Tecnologica and the Consiglio Nazionale delle Ricerche for financial support.

References and Notes

(1) Fichou, D. *Handbook of Oligo- and Polythiophenes*; Wiley: Chichester, UK, 1998.
(2) Muellen, K.; Wegner, G. *Electronic Materials: The Oligomer Approach*; Wiley: Chichester, UK, 1998.
(3) Roncali, J. *Chem. Rev.* **1997**, *97*, 173.
(4) Roncali, J. *Chem. Rev.* **1992**, *92*, 711.
(5) Brédas, J. L.; Themans, B.; Fripiat, J. G.;. Andrè, J. M. *Phys. Rev. B* **1984**, *29*, 6761.
(6) Skotheim, T. A. *Handbook of Conducting Polymers*; Marcel Dekker: New York, 1986; Vol. 1 and 2.
(7) Kuzmany, H.; Merhing, M.; Roth, S. *Electronic Properties of Conjugated Polymers*; Springer-Verlag: Berlin, 1987.
(8) Brédas, J.-L.; Chance, R. R. *Conjugated Polymeric Materials: Opportunities in Electronics, Optoelectronics and Molecular Electronics*; NATO ASI Series E, Vol. 182; Kluwer: Dordrecht, The Netherlands, 1990.
(9) Andrè, M.; Delhalle, J.; Brédas, J.-L. *Quantum Chemistry Aided Design of Organic Polymers*; World Scientific: Singapore, 1991.
(10) Jones, D.; Guerra, M.; Favaretto. L.; Modelli, A.; Fabrizio, M.; Distefano, G. *J. Phys. Chem.* **1990**, *94*, 5761.
(11) Distefano, G.: Jones, D.; Guerra, M.; Favaretto, L.; Modelli, A.; Mengoli, G. *J. Phys. Chem.* **1991**, *95*, 5761.
(12) Distefano, G.; Dal Colle, M.; Jones, D.; Zambianchi, M.; Favaretto, L.; Modelli, A. *J. Phys. Chem.* **1993**, *97*, 3504.
(13) Distefano, G.; de Palo, M.; Dal Colle, M.; Modelli A.; Jones, D.; Favaretto, L. *J. Mol. Struct. THEOCHEM* **1997**, *418*, 99.
(14) Distefano, G.; de Palo, M.; Dal Colle, M.; Guerra, M. *J. Mol. Struct. THEOCHEM* **1998**, *455*, 131.
(15) Dal Colle, M.; Cova, C.; Distefano, G.; Jones, D.; Modelli, A.; Comisso, N. *J. Phys. Chem.* **1999**, *103*, 2828.
(16) Tabor, B. J.; Boon, *J. Eur. Polym.* **1971**, *7*, 1127.
(17) Tripaty, S. K.; Kitchen, D.; Druy, M. A. *Macromolecules* **1983**, *16*, 190.
(18) Jones, T. P. H.; Mitchell, G. R,; Windle, A. H. *Colloid Polym. Sci.* **1983**, *261*, 110.
(19) Garbarczyk, J. *Polym. Commun.* **1986**, *27*, 335.
(20) Change, R. R.; Shacklette, L. W.; Eckhardt, H.; Sowa, J. M.; Elsenbaumer, R. L.; Ivory, D. M.; Miller, G. G.; Guy, R. III,; Baughman, R. H. *Polym. Sci. Technol.* **1981**, *15*, 125.
(21) Baughman, R. H.; Brédas, J. L.; Change, R. R.; Elsenbaumer, R. L.; Shacklette L. W. *Chem. Rev.* **1982**, *82*, 209.
(22) Duke, C. S.; Paton, A. *Org. Coat. Plast. Chem.* **1980**, *43*, 863.
(23) Brédas, J. L.; Change, R. R.; Baughman, R. H.; Silbey, R. *J. Chem. Phys.* **1983**, *76*, 3673.
(24) Rabolt, J. F.; Clarke, T. C.; Kanazawa, K. K.; Reynolds, J. R.; Street, G. B. *J. Chem. Soc. Chem. Commun.* **1980**, 347.
(25) Change, R. R.; Shacklette. L. W. Miller, G. G.; Ivory, D. M.; Sowa, J. M.; Elsenbaumer, R. L.; Baughman, R. H. *J. Chem. Soc. Chem. Commun.* **1980**, 348.
(26) Krivoshey, I. V.; Skorobogatov, V. M. *Polyacetylene and polyarylenes: Synthesis and Conductive Properties*; Gordon and Breach Science Publishers: Philadelphia, PA, 1991.
(27) Frommer, J. E. *Acc. Chem. Res.*, **1986**, *19*, 2.
(28) Heinrich, N.; Koch, W.; Frenking, G. *Chem Phys. Lett.* **1986**, *124*, 20.
(29) Dal Colle, M.; Distefano, G.; Modelli, A.; Jones, D.; Guerra, M.; Olivato, P. R.; da Silva Ribeiro, D. *J. Phys. Chem. A* **1998**, *102*, 8037.
(30) Modelli, A.; Scagnolari, F.; Jones, D.; Distefano, G. *J. Phys. Chem. A* **1998**, *103*, 9675.
(31) Modelli, A.; Scagnolari, F.; Distefano, G. *Chem. Phys.* **2000**, *250*, 311.
(32) Sanche, L.; Schulz, G. J. J. *Phys. Rev. A* **1972**, *5*, 1672.
(33) Modelli, A.; Jones, D.; Distefano, G. *Chem. Phys. Lett.* **1982**, *86*, 434.
(34) Johnston, A. R.; Burrow, P. D. *J. Electron Spectrosc. Relat. Phenom.* **1982**, *25*, 119.
(35) Frisch, M. J.; Trucks, G. W.; Schlegel, H. B.; Gill, P. M. W.; Johnson, B. G.; Robb, M. A.; Cheeseman, J. R.; Keith, T.; Petersson, G. A.; Montgomery, J. A.; Raghavachari, K.; Al- Laham, M. A.; Zakrzewski, V. G.; Ortiz, J. V.; Foresman, J. B.; Cioslowski, J.; Stefanov, B. B.; Nanayakkara, A.; Challacombe, M.; Peng, C. Y.; Ayala, P. Y.; Chen, W.; Wong, M. W.; Andres, J. L.; Replogle, E. S.; Gomperts, R.; Martin, R. L.; Fox, D. J.; Binkley, J. S.; Defrees, D. J.; Baker, J.; Stewart, J. P.; Head-Gordon, M.; Gonzales, C.; Pople, J. A. *Gaussian 94*, Revision D4; Gaussian, Inc.: Pittsburgh, PA, 1995.
(36) Schweig, A.; Thon, N. *Chem. Phys. Lett.* **1976**, *38*, 482.
(37) Distefano, G.; Guerra, M.; Jones, D.; Modelli, A. *Chem. Phys.* **1981**, *59*, 169.
(38) Wagner, G.; Bock, H. *Chem. Ber.* **1974**, *107*, 68.
(39) Bock, H.; Wagner, G. Kroner, J. *Chem. Ber.* **1972**, *105*, 3850.
(40) Kimura, K., Katsumata, S., Achiba, Y., Yamazaki, T., Iwata, S., Eds. *Handbook of He(I) Photoelectron Spectra of Fundamental Organic Molecules*; Japan Scientific Societies Press: Tokyo, 1981.
(41) Modelli, A.; Jones, D.; Distefano, G.; Tronc, M. *Chem. Phys. Lett.* **1991**, *181*, 361.
(42) Rabelais, J. W.; Colton, R. J. *J. Electron Spectrosc. Related Phenom.* **1972**, *1*, 80.
(43) Wentworth, W. E.; Kao, L. W.; Becker, R. S. *J. Phys. Chem.* **1975**, *79*, 1161.
(44) Giordan, J. C.; Moore, J. H.; Tossell, J. A.; Kaim, W. *J. Am. Chem. Soc.* **1985**, *107*, 5600.
(45) Modelli, A.; Jones, D.; Colonna, F. P.; Distefano, G. *Chem. Phys.* **1983**, *77*, 153.
(46) Dewar, P. S.; Ernstbrunner, E.; Gilmore, J. R.; Godfrey, M.; Mellor, J. M. *Tetrahedron* **1974**, *30*, 2455.
(47) Guerra, M.; Distefano, G.; Jones, D.; Colonna, F. P.; Modelli, A. *Chem. Phys.* **1984**, *91*, 383.
(48) Portaleone, G.; Domenicano, A.; Schultz, G.; Hargittai, *J. Mol. Struct.* **1987**, 60, 97.
(49) Lide, D. R. *Handbook of Chemistry and Physics*, 73rd ed.; CRC Press: Boca Raton, FL, 1992.
(50) Seip, H. M.; Seip R. *Acta Chem. Scand.* **1973**, *27*, 4024.
(51) Bondi, A. *J. Phys. Chem.* **1964**, *68*, 441.
(52) Burrow, P. D.; Howard, A. E.; Johnston, A. R.; Jordan, K. D. *J. Phys. Chem.* **1992**, *96*, 7570.
(53) Modelli, A.; Distefano, G.; Guerra, M.; Jones, D.; Rossini, S. *Chem. Phys. Lett.*, **1986**, *132*, 448.
(54) Distefano, G.; Dal Colle, M.; de Palo, M.; Jones, D.; Bombieri, G.; Del Pra, A.; Olivato, P. R.; Mondino, M. G. *J. Chem. Soc., Perkin Trans. 2* **1996**, 1661.
(55) Distefano, G.; Guerra, M.; Jones, D.; Modelli, A.; Colonna, F. P. *Chem. Phys.* **1980**, *52*, 389.
(56) Pignataro, S.; Distefano, G. *Z. Naturforsch.* **1975**, *30a*, 815.